ACS OMEGA

http://pubs.acs.org/journal/acsodf

Article

Golgi-Targeting Fluorescent Probe for Monitoring CO-Releasing Molecule-3 In Vitro and In Vivo

Songjiao Li, Ke Yang, Jiayu Zeng, Yiteng Ding, Dan Cheng, and Longwei He*

Cite This: *ACS Omega* 2022, 7, 9929−9935

Read Online

ACCESS | Metrics & More | Article Recommendations | Supporting Information

ABSTRACT: CO-releasing molecule-3 (CORM-3), mainly metal carbonyl compounds, is widely used as experimental tools to deliver CO, a biological "gasotransmitter", in mammalian systems. CORM-3 is also proposed as a potential new antimicrobial agent, which kills bacteria effectively and rapidly in vitro and in animal models. Organelle-targeting therapy, as a highly effective therapeutic strategy with little toxic and side effects, has important research significance and development prospects. Therefore, the development of effective methods for detecting and tracking CORM-3 at the subcellular level has important implications. In this paper, an easily available Golgi-targetable fluorescent probe (Golgi-Nap-CORM-3) was proposed for CORM-3 detection. In the probe Golgi-Nap-CORM-3, the phenyl sulfonamide group was selected as the Golgi-targetable unit, naphthalimide dye was chosen as a fluorophore, and the nitro group was selected as a CORM-3-responsive unit. Golgi-Nap-CORM-3 shows a CORM-3-reponsive increase of fluorescence emission at 520 nm. Using the excellent probe, the change of CORM-3 in HeLa cells, HepG2 cells, and zebrafish is successfully monitored. This study demonstrates very important information for the study of CORM-3 in vivo systems.

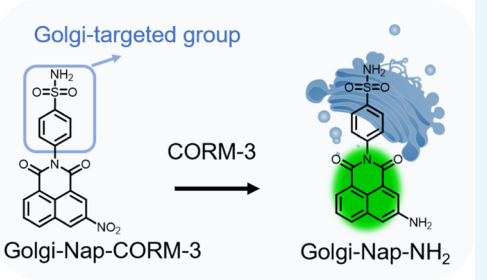

INTRODUCTION

CO-releasing molecule-3 (CORM-3), mainly metal carbonyl compounds, is widely used as experimental tools to deliver carbon monoxide (CO).[1−3] As a key endogenous gaseous signal molecule, CO shows great therapeutic potential for a variety of diseases, such as Alzheimer's disease,[4] hypertension,[5] inflammation,[6] heart failure,[7] and so on. However, due to the toxicity of CO by direct inhalation of CO gas, many problems exist in the treatment of diseases: uncontrollable problems and difficulties in targeted delivery.[8] Therefore, in the past decades, the development of appropriate CO-releasing molecules (CORMs) to replace CO gas for direct treatment of diseases has received extensive attention.[9] So far, many methods for detecting CO using CORM-3 as a CO donor have been developed, including chromogenic detection, electrochemical analysis, gas chromatography, and fluorescent assays.[10−12] Among these, because of its high sensitivity, imperial spatial resolution, noninvasive detection, technical simplicity, etc., fluorescent imaging has special advantage in monitoring the spatial and temporal distribution of analytes.[13−23] Recently, numerous innovative fluorescent probes have been reported for the visualization of CO using CORM-3 as a CO donor.[24−37]

As a vital organelle, the Golgi apparatus exists in most eukaryotic cells and plays a significant role in the internal membrane system. The Golgi is composed of a series of flattened cisternae, which are organized as ribbon stacks and closely linked with each other.[38] Under oxidative stress, proapoptotic, and DNA damage conditions, the complete structure and stable function of the Golgi apparatus might be damaged, resulting in Golgi fracture and cell apoptosis.[39,40] The Golgi apparatus has become a new choice for the research and treatment of oxidative stress-related diseases. Moreover, organelle-targeting therapy, as a highly effective therapeutic strategy with little toxic and side effects, has important research significance and development prospects. CORM-3 is proposed as a potential new antimicrobial agent that kills bacteria effectively and rapidly in vitro and in animal models.[41,42] The release of drugs through overexpression of CO in tumor cells provides a very excellent approach for the treatment of cancer. Thus, the development of CORM-3 as a prodrug for CO administration in organelle-targeting therapy has attracted significant attention. Unfortunately, no Golgi-specific fluorescent probe being capable of monitoring CORM-3 in living cells has been developed so far. The development of molecules that target the Golgi and image overexpressing CORM-3 in tumor cells has important implications for tumor therapy.

So far, three kinds of Golgi-targeting strategies have been used to realize Golgi targeting including Golgi-targeting polypeptides, cysteine, and sphingosine.[43−45] The methods

Received: January 20, 2022
Accepted: March 3, 2022
Published: March 11, 2022

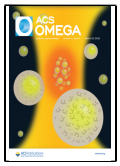

mentioned above have limitations in the synthesis of fluorescent probes. Therefore, it is urgent to develop a Golgi-targeting group, which should meet the following requirements: (1) accurate localization, (2) readily available raw materials, and (3) easy chemical modification.

Herein, we reported a simple-structure Golgi-targetable probe (Golgi-Nap-CORM-3) with easy synthetic steps for the detection of CORM-3. In the probe Golgi-Nap-CORM-3, the phenyl sulfonamide group was selected as the Golgi-targetable unit,[35−37] naphthalimide dye was chosen as a signal reporter, and the introduced nitro moiety in the fluorophore skeleton acts as a CO-responsive moiety (Scheme 1). The fluorescence

Scheme 1. Reaction Mechanism of the Probe Golgi-Nap-CORM-3 for the Detection of CORM-3

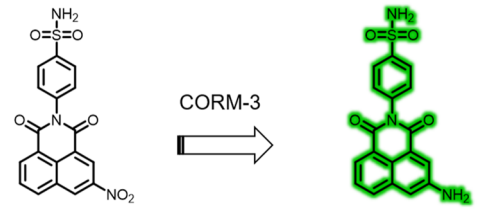

imaging indicated that Golgi-Nap-CORM-3 possesses an outstanding Golgi-targeting ability and was further applied to visualize the change of CORM-3 in HeLa cells, HepG2 cells, and zebrafish successfully.

EXPERIMENTAL SECTION

Reagents and Apparatus. Please see the Supporting Information for details.

Synthesis. Golgi-Nap-CORM-3 was synthesized according to the synthetic route described in Scheme S1.

Compound Golgi-Nap-CORM-3. The compounds 3-nitro-1,8-naphthalic anhydride (486 mg, 2 mmol) and sulfanilamide (344 mg, 2 mmol) were mixed in ethanol (15 mL). The mixture was heated and stirred at 80 °C for 12 h; then, reduced-pressure rotary distillation was performed. After that, a pale-yellow residue was obtained and purified using silica gel column chromatography (CH_2Cl_2/CH_3OH abluent, v/v = 20:1), to get a pure Golgi-Nap-CORM-3 (627 mg, 79%). ^{1}H NMR (400 MHz, DMSO-d_6, Figure S1) δ 9.56 (s, 1H), 8.97 (s, 1H), 8.86 (d, J = 6.8 Hz, 1H), 8.72 (d, J = 6 Hz, 1H), 8.11 (t, J = 6.0 Hz, 1H), 8.02 (d, J = 6.8 Hz, 2H), 7.66 (d, J = 6.8 Hz, 2H), 7.55 (s, 2H). ^{13}C NMR (100 MHz, DMSO-d_6, Figure S2) δ 163.5, 163.0, 146.3, 144.6, 139.1, 137.0, 134.4, 131.5, 130.5, 130.4, 130.3, 129.8, 127.0, 125.0, 123.6, 123.3. HRMS (ESI, Figure S3): $[M + H]^+$ calcd. 398.0447, found 398.0440.

Spectroscopic Measurements. For the probe Golgi-Nap-CORM-3, its stock solution was made in DMSO with a concentration of 1 mM. In total, a 10.0 μL stock solution was mixed into 1.0 mL of pH 7.4 phosphate buffer solution (10 mM) in the titration experiments to keep the final Golgi-Nap-CORM-3 concentration at 10 μM. CORM-3 solution was made in twice-distilled water and further diluted. A total of 10 μL of Golgi-Nap-CORM-3 stock solution was added to 1.0 mL of pH 7.4 phosphate buffer solution (10 mM) followed by the addition of different volumes of CORM-3 solution. The excitation wavelength was recorded at 430 nm, and the collection wavelength range was from 450 to 700 nm. A slit width of Ex/Em = 5/5 nm was set for all fluorescence spectral measurements.

Cell Culture. HeLa and HepG2 cells were cultured in Dulbecco's modified Eagle medium including 10% fetal bovine serum at 37 °C with 5% CO_2 in a humidified atmosphere.

Cytotoxicity Assays. Cytotoxicity of probe was characterized using 3-(4,5-dimethylthiazol-2-yl)-2,5-diphenyltetrazolium bromide (MTT) assay. HeLa or HepG2 cells were seeded into a 96-well plate at 3×10^3/well. They were cultured at 37 °C under 5% CO_2 for 24 h. Then, the cells were treated with 1, 5, 10, 20, or 30 μM Golgi-Nap-CORM-3 for 4 h. MTT (5 mg/mL in PBS) was added into each well and incubated for another 4 h. Then, in DMSO (150 μL/well), formazan was dissolved. The absorption was recorded at 490 nm. Before the experiment, the HeLa cells were transferred to confocal dishes for attachment and growth. The mixture was cultured at 37 °C overnight; then, the original medium was removed and washed with PBS twice. Then, Golgi-Nap-CORM-3 (10 μM) was added in DMEM into the dish, and the cells were incubated at 37 °C under 5% CO_2 for 1 h. After that, the cells were washed with PBS to remove the residual probe, and the CORM-3 solution (50 μM) was added into the dishes. This was incubated for another 1 h; then, the cells were washed with PBS. A total of 500 nM Golgi Tracker Red was added to the dish and incubated at 37 °C under 5% CO_2 for 15 min.

Cell Treatment and Cell Imaging. For the exogenous CO imaging in living cells, HeLa or HepG2 cells were incubated with 10 μM Golgi-Nap-CORM-3 for 1 h at 37 °C; then, the media were replaced with PBS buffer. The cells were treated with different concentrations of CORM-3 (0, 20, 40, 60, and 80 μM) for 1 h. Before observation, the cells were washed three times with PBS. The images were acquired with a 458 nm excitation and emission collection range of 481−580 nm.

Zebrafish Maintenance and Imaging. The wild-type zebrafish larvae (purchased from Shanghai Fish Bio Co., Ltd.) were incubated with E3 embryo medium at 28 °C. For imaging, 3 day old larvae were transferred into a 6-well microplate using a disposable transfer pipette. The larvae were incubated with Golgi-Nap-CORM-3 (10 μM) for 1 h. Then, the zebrafish was treated with CORM-3 (0 or 80 μM) for another 1 h. Then, the zebrafish were anesthetized, and zebrafish imaging was conducted on a confocal laser scanning microscope. The images were acquired with a 458 nm excitation and emission collection range of 481−580 nm.

RESULTS AND DISCUSSION

Spectral Response of Golgi-Nap-CORM-3 to CORM-3. Using the Golgi-targetable fluorescent probe Golgi-Nap-CORM-3, we first studied the sensing ability of Golgi-Nap-CORM-3 with different concentrations (0−80 μM) of CORM-3. First, the probe emitted a faint emission band at 520 nm due to the strong electron-withdrawing ability of the nitro group. Addition of increasing concentration of CORM-3, a new emission band centered at 520 nm was generated obviously, and the intensity increased with increasing concentration of CORM-3 (Figure 1). When CORM-3 concentration increases to 80 μM, and the signal enhancement occurred 32 times. The inset of Figure 1 shows that the fluorescent intensity of Golgi-Nap-CORM-3 at 520 nm improved linearly with CORM-3 ranging within 0.5−80 μM, and the probe detection limit for CORM-3 was calculated to be 0.35 μM (3σ/slope). These results show that Golgi-Nap-CORM-3 is a useful fluorescent

https://doi.org/10.1021/acsomega.2c00422
ACS Omega 2022, 7, 9929−9935

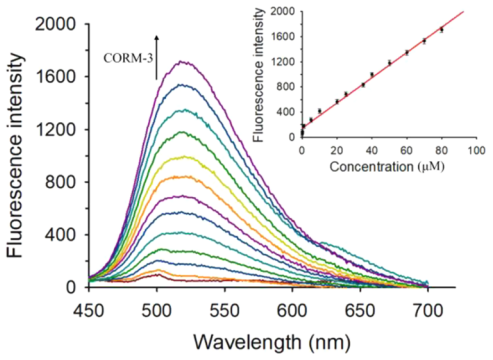

Figure 1. Fluorescence spectra of Golgi-Nap-CORM-3 (10 μM) upon incubation with a series of concentrations of CORM-3 (0, 0.5, 1, 5, 10, 20, 25, 35, 40, 50, 60, 70, and 80 μM, 37 °C) for 60 min. Inset: the curve was plotted with the probe fluorescence intensity (FI) vs CORM-3 concentration. λ_{ex} = 430 nm.

"turn on" probe with a high signal-to-noise ratio for the CORM-3 detection. In addition, the optical response of Golgi-Nap-CORM-3 to CORM-3 was examined by measuring its absorption spectral changes. As shown in Figure S4, upon the addition of CORM-3 to the probe Golgi-Nap-CORM-3, a new red-shifted absorption band centered at 440 nm was significantly generated.

To further explain the CORM-3-reponsive emission and absorption spectral changes, we employed time-dependent density functional theory (TD-DFT) to calculate the molecular frontier orbit of the probe and separate components (naphthalimide fluorophore, and nitro and amino groups) using Gaussian 09 programs (B3LYP/6-31G). The highest occupied molecular orbital (HOMO) and lowest occupied molecular orbital (LUMO) were characterized on the probe Golgi-Nap-CORM-3 and its amino product (Golgi-Nap-NH_2). As expected, the HOMO−LUMO energy gap of Golgi-Nap-NH_2 (3.52 eV) is smaller than that of the probe (3.96 eV) (Figure 2A), which gave rise to the generation of a new red-shifted absorption band because of the intramolecular charge transfer (ICT) process activation. In addition, as shown in Figure 2B, the LUMO energy level of the nitro moiety (−3.41 eV) is positioned between the HOMO (−6.86 eV) and LUMO (−2.87 eV) energy levels of the naphthalimide fluorophore, which results in that its fluorescence could be quenched by a donor-excited photoinduced electron transfer (d-PET) mechanism. Compared with the nitro group, the LUMO energy level of the amino moiety increases to 0.06 eV, which is higher than that of the naphthalimide moiety. Accordingly, the reduction of nitro to amine on the compound Golgi-Nap-CORM-3 could block the PET process and induce fluorescence enhancement. Thus, the spectral response of the probe toward CORM-3 is regulated by collaborative ICT and PET mechanisms.[38] In addition, the result of high-resolution mass spectrometry indicated that the reaction of Golgi-Nap-CORM-3 with CORM-3 yielded the amino product (Golgi-Nap-NH_2, HRMS: $[M + H]^+$ calcd. 368.0705, found 368.0698) (Figure S5).

Furthermore, we investigated the Golgi-Nap-CORM-3 fluorescence selectivity toward various potentially activated species. As illustrated in Figure 3, only CORM-3 could open strong fluorescence emission; other biologically relevant analytes, including reactive oxygen species, reactive nitrogen species, reactive sulfur species, reducing species, common

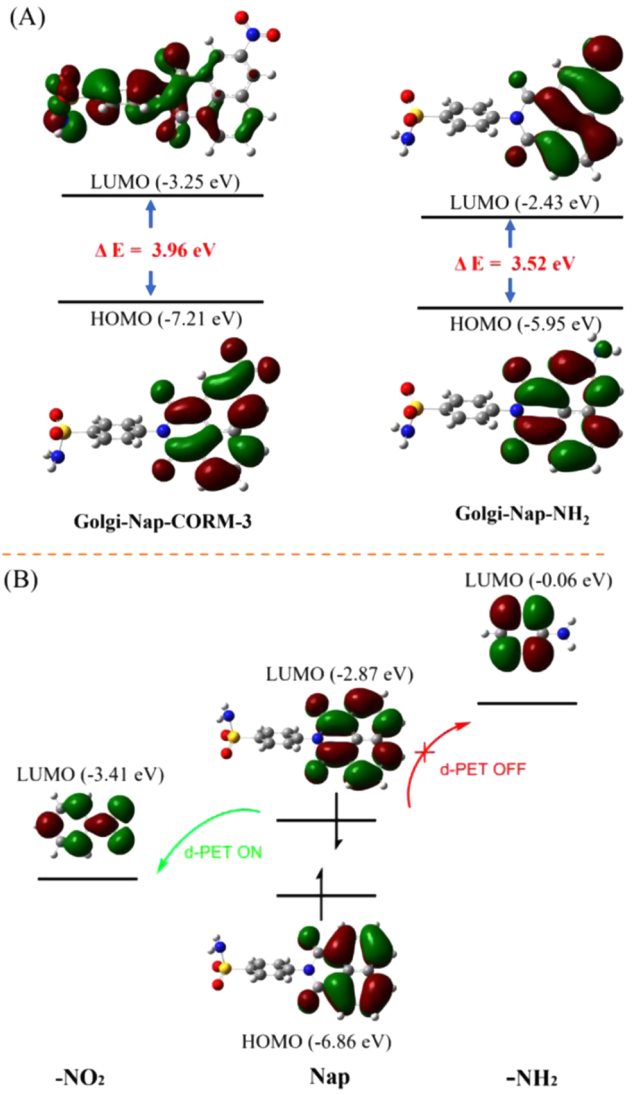

Figure 2. Frontier orbital diagrams of (A) compounds Golgi-Nap-CORM-3 and Golgi-Nap-NH_2 and (B) separate naphthalimide, nitro, and amino units.

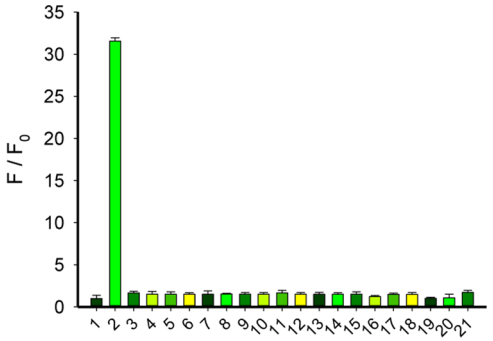

Figure 3. Selectivity of Golgi-Nap-CORM-3 (10 μM) toward various analytes (100 μM, except 500 μM Cys, Hcy and 1 mM GSH). (1, Blank; 2, CORM-3; 3, H_2O_2; 4, $^{\bullet}OH$; 5, $^1O_2$; 6, ClO^-; 7, $O_2^{\bullet-}$; 8, $ONOO^-$; 9, NO; 10, GSH; 11, Cys; 12, Hcy; 13, H_2S; 14, Vc; 15, Fe^{2+}; 16, Fe^{3+}; 17, Cu^{2+}; 18, Zn^{2+}; 19, HCO_3^-; 20, CO_3^{2-}; and 21, SO_4^{2-}.) λ_{ex} = 430 nm.

cations, and common anions, had negligible interference in the fluorescence of Golgi-Nap-CORM-3 under the same con-

https://doi.org/10.1021/acsomega.2c00422
ACS Omega 2022, 7, 9929−9935

ditions. Therefore, the probe Golgi-Nap-CORM-3 possessed high selectivity to detect CORM-3.

To examine the practicability of the new probe (Golgi-Nap-CO), the pH effect was also explored. As Figure S6 indicates, without CORM-3, the free probe's FI shows faint and stable fluorescence emission with pH 5.5−8.0, showing that the pH changes have little influences on the free probe, while upon addition of CORM-3, the FI increased significantly, especially under the physiological conditions (pH 7.4), which is key to its biological application.

To further demonstrate the sensitivity of Golgi-Nap-CORM-3 toward CORM-3, the time-dependent FI changes of Golgi-Nap-CORM-3 reacting with CORM-3 at various concentrations (0, 20, 40, 60, and 80 μM) were checked, and the results are displayed in Figure 4. Upon additions of increased

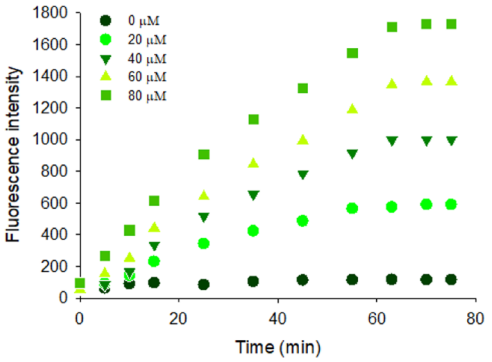

Figure 4. Time-dependent intensity of Golgi-Nap-CORM-3 (10 μM) at 520 nm after addition of concentrations of CORM-3 (0, 20, 40, 60, and 80 μM). λ_{ex} = 430 nm.

concentrations of CORM-3, the FI of Golgi-Nap-CORM-3 at 520 nm increased and reached a plateau after 60 min. Without CORM-3, no obvious change in FI at 520 nm was observed. It further proves that the probe Golgi-Nap-CORM-3 can sensitively detect CORM-3. As additional controls, we added CO gas to the probe solution and did not see any fluorescent changes. We also detected the CORM-2-emissive response; although the remarkable enhancement of fluorescent intensity at 520 nm was generated, it is much weaker than that induced by CORM-3 (Figure S7). Therefore, the probe Golgi-Nap-CORM-3 exhibits better selectivity for CORM-3 over CORM-2.

Cytotoxic Effect of Golgi-Nap-CORM-3. The cytotoxicity of the probe Golgi-Nap-CORM-3 was evaluated before imaging in living cells. The cytotoxicity of Golgi-Nap-CORM-3 was investigated in HeLa and HepG2 cells through MTT assay (Figures S8 and S9). In addition, the visual maps to show the cytotoxicity are shown in Figures S10 and S11. More than 85% cell viability is found after the cells were incubated for 24 h with different concentrations of Golgi-Nap-CORM-3 (0−30 μM). These results showed that Golgi-Nap-CORM-3 had low cytotoxicity to cells under our experimental conditions. Moreover, the *n*-octanol/water partition coefficient (log *P*) of Golgi-Nap-CORM-3 was calculated as 2.61. This result indicated that Golgi-Nap-CORM-3 has good cell permeability.

Colocalization Imaging in Living Cells. Due to the phenyl sulfonamide moiety in Golgi-Nap-CORM-3, we anticipated that the sensor has Golgi targeting properties. Therefore, we performed the subcellular localization experiment in HeLa cells to investigate whether the probe Golgi-Nap-CORM-3 can selectively localize in the Golgi (Figure 5). HeLa cells were coincubated with Golgi-Nap-CORM-3/CORM-3 and Golgi Tracker Red (a commercial Golgi tracker). The cells showed green fluorescence for the probe (Figure 5a) and red fluorescence for Golgi Tracker Red (Figure 5b). The merged image indicates that the probe overlapped well with Golgi Tracker Red (Figure 5c). The cells' bright field is shown in Figure 5d,e. In addition, the intensity scatter plot has an excellent overlap and Pearson's colocalization coefficient (0.93, Figure 5f). According to reports in the literature, COX-2 has been used as an excellent traceable biomarker and exists maximally in the Golgi apparatus whether the organelles are damaged or not. Therefore, the damaged or nondamaged Golgi apparatus does not affect the target function of the phenyl sulfonamide group. As designed, the probe targeted the Golgi specifically.

Visualizing CORM-3 in Living Cells. Because of the excellent performance of Golgi-Nap-CORM-3, the potential applications of Golgi-Nap-CORM-3 for CO imaging in living cells were studied. In Figure 6, when HeLa cells were stained

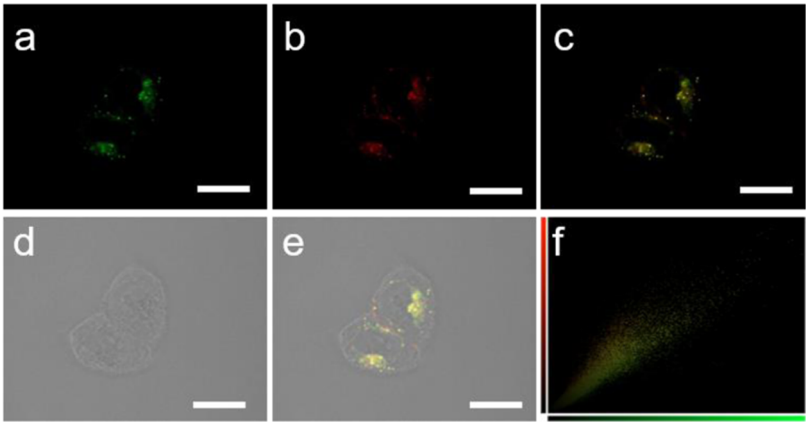

Figure 5. Colocalization fluorescence images of HeLa cells coincubated with Golgi-Nap-CORM-3 (10 μM), CORM-3 (50 μM), and Golgi Tracker Red (500 nM). (a) HeLa cells incubated with CORM-3 for 1 h, followed by treatment with Golgi-Nap-CORM-3 for 1 h in the green channel, λ_{ex} = 458 nm, collected at 481−580 nm. (b) HeLa cells stained with Golgi Tracker Red (500 nM) for 0.5 h in the red channel, λ_{ex} = 561 nm, collected at 580−620 nm. (c) Merged image of (a) and (b). (d) Bright-field image. (e) Merged image of (a)−(d). (f) Intensity scatter plot of the green channel and the red channel. Scale bars are 20 μm.

https://doi.org/10.1021/acsomega.2c00422
ACS Omega 2022, 7, 9929−9935

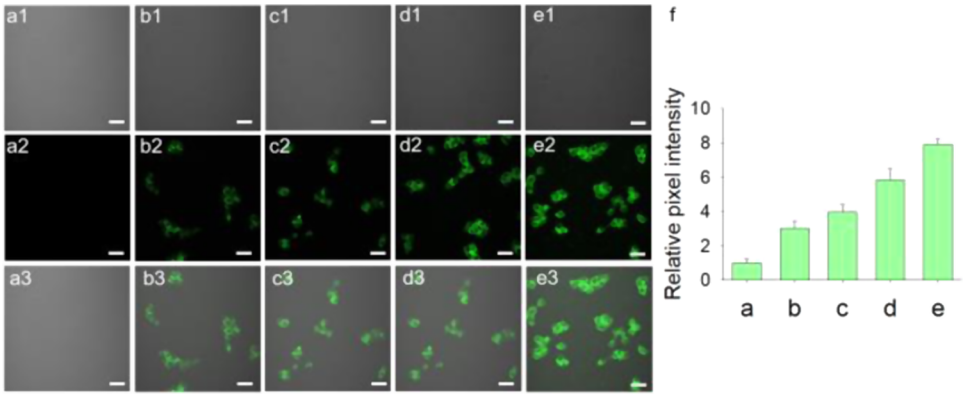

Figure 6. Confocal fluorescence images of HeLa cells. (a−e) Cells incubated with different concentrations of CORM-3 (0, 20, 40, 60, and 80 μM) for 1 h, followed by treatment with 10 μM Golgi-Nap-CORM-3 for 1 h. (f) Relative FI of (a)−(e). λ_{ex} = 458 nm, collected at 481−580 nm. Scale bar: 20 μm.

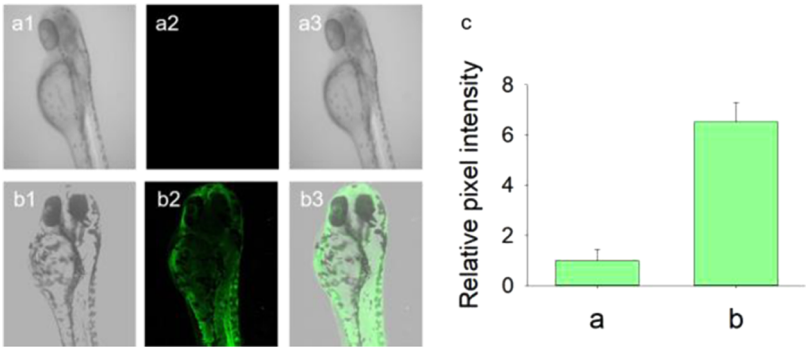

Figure 7. Confocal fluorescence images of zebrafish. (a) Zebrafish treatment with 10 μM Golgi-Nap-CORM-3 for 1 h. (b) Zebrafish incubated with 80 μM CORM-3 for 1 h, followed by treatment with 10 μM Golgi-Nap-CORM-3 for 1 h. (c) Relative FI of (a) and (b). λ_{ex} = 458 nm, collected at 481−580 nm.

with only the probe, almost no fluorescence was found in the green channel. However, when cells were exposed to increasing concentrations of CORM-3 (20, 40, 60, and 80 μM), the cells exhibited green fluorescence, and the FI was dose-related to the CORM-3 concentration. In addition, as shown in Figure 6, the fluorescence enhancement was observed for 1 h, which suggests that Golgi-Nap-CORM-3 has good chemical stability that can be used to monitor CORM-3 in living cells for a long time and is not easily affected by metabolism. These data displayed that our probe Golgi-Nap-CORM-3 has good permeability. Similar results were also found in HepG-2 cells (Figure S12). All of these data suggest that Golgi-Nap-CORM-3 is sensitive to track exogenous CO.

Visualizing CORM-3 in Living Zebrafish. We further explore the performance of Golgi-Nap-CORM-3 for detection of CO in zebrafish models. When the zebrafish were stained with only the probe Golgi-Nap-CORM-3 for 1 h, almost no fluorescence signal was collected (Figure 7a), while after the zebrafish were treated with 80 μM CORM-3 and then incubated with Golgi-Nap-CORM-3, green fluorescence increased obviously (Figure 7b,c), indicating that Golgi-Nap-CORM-3 was organism-permeable and extraordinarily sensitive for living sample imaging.

CONCLUSIONS

In summary, a readily available Golgi-targetable fluorescent probe Golgi-Nap-CORM-3 for the imaging of CORM-3 was developed. It exhibits excellent fluorescent response, such as large coinduced signal enhancement (32-fold), a low detection limit (0.35 μM), and high selectivity. The CORM-3 change in HeLa cells, HepG2 cells, and zebrafish is also successfully monitored using Golgi-Nap-CORM-3. This probe opened a new way to produce an easily available Golgi probe for visualization of CORM-3 in real time in a living system and provides an effective method for deeper learning of the roles of CORM-3, which is considered to be a potential new antimicrobial agent, in physiological/pathological processes. We expect Golgi-Nap-CORM-3 to become an important tool for the exploration of ideal CO treatment drugs in future medicine.

ASSOCIATED CONTENT

Supporting Information

The Supporting Information is available free of charge at https://pubs.acs.org/doi/10.1021/acsomega.2c00422.

^{1}H NMR, ^{13}C NMR, and MS spectra, additional spectroscopic data, cell cytotoxicity, and supplemental fluorescence images of cells (PDF)

AUTHOR INFORMATION

Corresponding Author

Longwei He − *Cancer Research Institute, Hunan Province Cooperative Innovation Center for Molecular Target New Drug Study, Department of Pharmacy and Pharmacology, Hengyang Medical School, University of South China,*

https://doi.org/10.1021/acsomega.2c00422
ACS Omega 2022, 7, 9929−9935

Hengyang 421001, China; orcid.org/0000-0002-8206-8783; Email: helongwei0110@163.com

Authors

Songjiao Li − *Cancer Research Institute, Hunan Province Cooperative Innovation Center for Molecular Target New Drug Study, Department of Pharmacy and Pharmacology, Hengyang Medical School, University of South China, Hengyang 421001, China*

Ke Yang − *Cancer Research Institute, Hunan Province Cooperative Innovation Center for Molecular Target New Drug Study, Department of Pharmacy and Pharmacology, Hengyang Medical School, University of South China, Hengyang 421001, China*

Jiayu Zeng − *Cancer Research Institute, Hunan Province Cooperative Innovation Center for Molecular Target New Drug Study, Department of Pharmacy and Pharmacology, Hengyang Medical School, University of South China, Hengyang 421001, China*

Yiteng Ding − *Clinical Research Institute, The Affiliated Nanhua Hospital, Hengyang Medical School, University of South China, Hengyang 421001, China*

Dan Cheng − *Clinical Research Institute, The Affiliated Nanhua Hospital, Hengyang Medical School, University of South China, Hengyang 421001, China; State Key Laboratory of Chemo/Biosensing and Chemometrics, College of Chemistry and Chemical Engineering, Hunan University, Changsha 410000, China*

Complete contact information is available at: https://pubs.acs.org/10.1021/acsomega.2c00422

Notes

The authors declare no competing financial interest.

■ ACKNOWLEDGMENTS

This work was supported by the National Natural Science Foundation of China (21904035), China Postdoctoral Science Foundation (2020T130184), the Hunan Provincial Natural Science Foundation of China (2020JJ5033), the Science and Technology Project of Hunan Province (2021RC3108), and start-up funds of the University of South China (201RGC012).

■ REFERENCES

(1) Clark, J. E.; Naughton, P.; Shurey, S.; Green, C.-J.; Johnson, T.-R.; Mann, B.-E.; Foresti, R.; Motterlini, R. Cardioprotective actions by a water-soluble carbon monoxide-releasing molecule. *Circ. Res.* **2003**, *93*, e2−e8.

(2) Foresti, R.; Hammad, J.; Clark, J. E.; Johnson, T. R.; Mann, B. E.; Friebe, A.; Green, C. J.; Motterlini, R. Vasoactive properties of CORM-3, a novel water-soluble carbon monoxide-releasing molecule. *Br. J. Pharmacol.* **2004**, *142*, 453−460.

(3) Michel, B. W.; Lippert, A. R.; Chang, C. J. A reaction-based fluorescent probe for selective imaging of carbon monoxide in living cells using a palladium-mediated carbonylation. *J. Am. Chem. Soc.* **2012**, *134*, 15668−15671.

(4) Choi, Y. K. Role of CO-releasing molecule-3 in Neurovascular Repair Processing. *Biomol. Ther.* **2018**, *26*, 93−100.

(5) Rose, L.; Prins, K. W.; Archer, S. L.; Pritzker, M.; Weir, E. K.; Misialek, J. R.; Thenappan, T. Survival in pulmonary hypertension due to chronic lung disease: Influence of low diffusion capacity of the lungs for CO-releasing molecule-3. *J. Heart Lung Transplant.* **2019**, *38*, 145−155.

(6) Lee, I. T.; Luo, S. F.; Lee, C. W.; Wang, S. W.; Lin, C. C.; Chang, C. C.; Chen, Y. L.; Chau, L. Y.; Yang, C. M. Overexpression of HO-1 protects against TNF-alpha-mediated airway inflammation by down-regulation of TNFR1-dependent oxidative stress. *Am. J. Pathol.* **2009**, *175*, 519−532.

(7) Reboul, C.; Boissière, J.; André, L.; Meyer, G.; Bideaux, P.; Fouret, G.; Feillet-coudray, C.; Obert, P.; Lacampagne, A.; Thireau, J.; Cazorla, O.; Richard, S. Carbon monoxide pollution aggravates ischemic heart failure through oxidative stress pathway. *Sci. Rep.* **2017**, *7*, No. 39715.

(8) Foresti, R.; Bani-Hani, M. G.; Motterlini, R. Use of carbon monoxide as a therapeutic agent: promises and challenges. *Intensive Care Med.* **2008**, *34*, 649−658.

(9) García-Gallego, S.; Bernardes, G. J. Carbon-monoxide-releasing molecules for the delivery of therapeutic CO in vivo. *Angew. Chem., Int. Ed.* **2014**, *53*, 9712−9721.

(10) Moragues, M. E.; Esteban, J.; Ros-Lis, J. V.; Martinez-Manez, R.; Marcos, M. D.; Martinez, M.; Soto, J.; Sancenon, F. Sensitive and selective chromogenic sensing of carbon monoxide via reversible axial CO coordination in binuclear rhodium complexes. *J. Am. Chem. Soc.* **2011**, *133*, 15762−15772.

(11) Park, S. S.; Kim, J.; Lee, Y. Improved electrochemical microsensor for the real-time simultaneous analysis of endogenous nitric oxide and carbon monoxide generation. *Anal. Chem.* **2012**, *84*, 1792−1796.

(12) Gras, R.; Hua, Y.; Luong, J.; Qiao, P.; Yang, X. G.; Yang, P. Metal 3D-printed catalytic jet and flame ionization detection for in situ trace carbon oxides analysis by gas chromatography. *J. Sep. Sci.* **2019**, *42*, 2826−2834.

(13) Yang, M.; Fan, J.; Du, J.; Peng, X. Small-molecule fluorescent probes for imaging gaseous signaling molecules: current progress and future implications. *Chem. Sci.* **2020**, *11*, 5127−5141.

(14) Gao, P.; Pan, W.; Li, N.; Tang, B. Fluorescent probes for organelle-targeted bioactive species imaging. *Chem. Sci.* **2019**, *10*, 6035−6071.

(15) Dou, K.; Huang, W.; Xiang, Y.; Li, S.; Liu, Z. Design of Activatable NIR-II Molecular Probe for In Vivo Elucidation of Disease-Related Viscosity Variations. *Anal. Chem.* **2020**, *92*, 4177−4181.

(16) Cheng, D.; Xu, W.; Gong, X.; Yuan, L.; Zhang, X. B. Design Strategy of Fluorescent Probes for Live Drug-Induced Acute Liver Injury Imaging. *Acc. Chem. Res.* **2021**, *54*, 403−415.

(17) He, L.; Yang, Y.; Lin, W. Rational Design of a Rigid Fluorophore-Molecular Rotor-Based Probe for High Signal-to-Background Ratio Detection of Sulfur Dioxide in Viscous System. *Anal. Chem.* **2019**, *91*, 15220−15228.

(18) Xiong, J.; Wang, W.; Wang, C.; Zhong, C.; Ruan, R.; Mao, Z.; Liu, Z. Visualizing Peroxynitrite in Microvessels of the Brain with Stroke Using an Engineered Highly Specific Fluorescent Probe. *ACS Sens.* **2020**, *5*, 3237−3245.

(19) Yu, X.; Xiang, L.; Yang, S.; Qu, S.; Zeng, X.; Zhou, Y.; Yang, R. A near-infrared fluorogenic probe with fast response for detecting sodium dithionite in living cells. *Spectrochim. Acta, Part A* **2021**, *245*, No. 118887.

(20) Zhang, Y.; Zhang, X.; Yang, H.; Yu, L.; Xu, Y.; Sharma, A.; Yin, P.; Li, X.; Kim, J. S.; Sun, Y. Advanced biotechnology-assisted precise sonodynamic therapy. *Chem. Soc. Rev.* **2021**, *50*, 11227−11248.

(21) Tuo, W.; Xu, Y.; Fan, Y.; Li, J.; Qiu, M.; Xiong, X.; Li, X.; Sun, Y. Biomedical applications of Pt(II) metallacycle/metallacage-based agents: From mono-chemotherapy to versatile imaging contrasts and theranostic platforms. *Coord. Chem. Rev.* **2021**, *443*, No. 214017.

(22) Xu, Y.; Tuo, W.; Yang, L.; Sun, Y.; Li, C.; Chen, X.; Yang, W.; Yang, G.; Stang, P. J.; Sun, Y. Design of a Metallacycle-Based Supramolecular Photosensitizer for In Vivo Image-Guided Photodynamic Inactivation of Bacteria. *Angew. Chem., Int. Ed.* **2022**, *61*, No. e202110048.

(23) Li, C.; Liu, C.; Fan, Y.; Ma, X.; Zhan, Y.; Lu, X.; Sun, Y. Recent development of near-infrared photoacoustic probes based on small-molecule organic dye. *RSC Chem. Biol.* **2021**, *2*, 743−758.

(24) Liu, K.; Kong, X.; Ma, Y.; Lin, W. Rational Design of a Robust Fluorescent Probe for the Detection of Endogenous carbon monoxide

in Living Zebrafish Embryos and Mouse Tissue. *Angew. Chem., Int. Ed.* **2017**, *56*, 13489−13492.
(25) Li, Y.; Wang, X.; Yang, J.; Xie, X.; Li, M.; Niu, J.; Tong, L.; Tang, B. Fluorescent Probe Based on Azobenzene-Cyclopalladium for the Selective Imaging of Endogenous CO-releasing molecule-3 under Hypoxia conditions. *Anal. Chem.* **2016**, *88*, 11154−11159.
(26) Zheng, K.; Lin, W.; Tan, L.; Chen, H.; Cui, H. A unique carbazole−coumarin fused two-photon platform: development of a robust two-photon fluorescent probe for imaging carbon monoxide in living tissues. *Chem. Sci.* **2014**, *5*, 3439−3448.
(27) Wang, J.; Li, C.; Chen, Q.; Li, H.; Zhou, L.; Jiang, X.; Shi, M.; Zhang, P.; Jiang, G.; Tang, B. Z. An Easily Available Ratiometric Reaction-Based AIE Probe for CO-releasing molecule-3 Light-up Imaging. *Anal. Chem.* **2019**, *91*, 9388−9392.
(28) Feng, W.; Feng, S.; Feng, G. A Fluorescent ESIPT Probe for Imaging CO-Releasing Molecule-3 in Living Systems. *Anal. Chem.* **2019**, *91*, 8602−8606.
(29) Tian, Y.; Jiang, W. L.; Wang, W. X.; Peng, J.; Li, X. M.; Li, Y.; Li, C. Y. The construction of a near-infrared fluorescent probe with dual advantages for imaging carbon monoxide in cells and in vivo. *Analyst* **2021**, *146*, 118−123.
(30) Jiang, W. L.; Wang, W. X.; Mao, G. J.; Yan, L.; Du, Y.; Li, Y.; Li, C. Y. construction of NIR and Ratiometric Fluorescent Probe for Monitoring carbon monoxide under Oxidative Stress in Zebrafish. *Anal. Chem.* **2021**, *93*, 2510−2518.
(31) Xia, Y.-S.; Yan, L.; Mao, G.-J.; Jiang, W.-L.; Wang, W.-X.; Li, Y.; Jiang, Y.-Q.; Li, C.-Y. A novel HPQ-based fluorescent probe for the visualization of carbon monoxide in zebrafish. *Sens. Actuators, B* **2021**, *340*, No. 129920.
(32) Robson, J. A.; Kubankova, M.; Bond, T.; Hendley, R. A.; White, A. J. P.; Kuimova, M. K.; Wilton-Ely, J. Simultaneous Detection of carbon monoxide and Viscosity Changes in Cells. *Angew. Chem., Int. Ed.* **2020**, *59*, 21431−21435.
(33) Li, S. J.; Zhou, D. Y.; Li, Y. F.; Yang, B.; Ou-Yang, J.; Jie, J.; Liu, J.; Li, C. Y. Mitochondria-targeted near-infrared fluorescent probe for the detection of carbon monoxide in vivo. *Talanta* **2018**, *188*, 691−700.
(34) Zhang, C.; Xie, H.; Zhan, T.; Zhang, J.; Chen, B.; Qian, Z.; Zhang, G.; Zhang, W.; Zhou, J. A new mitochondrion targetable fluorescent probe for carbon monoxide specific detection and live cell imaging. *Chem. Commun.* **2019**, *55*, 9444−9447.
(35) Dhara, K.; Lohar, S.; Patra, A.; Roy, P.; Saha, S. K.; Sadhukhan, G. C.; Chattopadhyay, P. A new lysosome-targetable turn-on fluorogenic probe for carbon monoxide imaging in living cells. *Anal. Chem.* **2018**, *90*, 2933−2938.
(36) Lazarus, L. S.; Benninghoff, A. D.; Berreau, L. M. Development of Triggerable, Trackable, and Targetable Carbon Monoxide Releasing Molecules. *Acc. Chem. Res.* **2020**, *53*, 2273−2285.
(37) Li, Z.; Jia, X.; Zhang, P.; Guo, Z.; Zhao, H.; Li, X.; Wei, C. A hepatocyte-specific fluorescent probe for imaging endogenous carbon monoxide release in vitro and in vivo. *Sens. Actuators, B* **2021**, *344*, No. 130177.
(38) Hicks, S. W.; Machamer, C. E. Golgi structure in stress sensing and apoptosis. *Biochim. Biophys. Acta* **2005**, *1744*, 406−414.
(39) Jiang, Z.; Hu, Z.; Zeng, L.; Lu, W.; Zhang, H.; Li, T.; Xiao, H. The role of the Golgi apparatus in oxidative stress: is this organelle less significant than mitochondria. *Free Radical Biol. Med.* **2011**, *50*, 907−917.
(40) Nakagomi, S.; Barsoum, M. J.; Bossy-Wetzel, E.; Sütterlin, C.; Malhotra, V.; Lipton, S. A. A Golgi fragmentation pathway in neurodegeneration. *Neurobiol. Dis.* **2008**, *29*, 221−231.
(41) Mann, B. E. CO-Releasing Molecules: A Personal View. *Organometallics* **2012**, *31*, 5728−5735.
(42) Romão, C. C.; Blättler, W. A.; Seixas, J. D.; Bernardes, G. J. Developing drug molecules for therapy with carbon monoxide. *Chem. Soc. Rev.* **2012**, *41*, 3571−3583.
(43) Srikun, D.; Albers, A. E.; Nam, C. I.; Iavarone, A. T.; Chang, C. J. Organelle-Targetable Fluorescent Probes for Imaging Hydrogen Peroxide in Living Cells via SNAP-Tag Protein Labeling. *J. Am. Chem. Soc.* **2010**, *132*, 4455−4465.
(44) Li, R. S.; Gao, P. F.; Zhang, H. Z.; Zheng, L. L.; Li, C. M.; Wang, J.; Li, Y. F.; Liu, F.; Li, N.; Huang, C. Z. Chiral nanoprobes for targeting and long-term imaging of the Golgi apparatus. *Chem. Sci.* **2017**, *8*, 6829−6835.
(45) Fan, L.; Wang, X.; Ge, J.; Li, F.; Zhang, C.; Lin, B.; Shuang, S.; Dong, C. A Golgi-targeted off-on fluorescent probe for real-time monitoring of pH changes in vivo. *Chem. Commun.* **2019**, *55*, 6685−6688.

https://doi.org/10.1021/acsomega.2c00422
ACS Omega 2022, 7, 9929−9935